PREDICTING PHASE EQUILIBRIA OF SPINEL-FORMING CONSTITUENTS IN WASTE GLASS SYSTEMS

Theodore M. Besmann and Nagraj S. Kulkarni
Metals and Ceramics Division
Oak Ridge National Laboratory
Oak Ridge, TN 37831-6063

Karl E. Spear
44 Tidnish Head Road, RR#2
Amherst, NS B4H 3X9 Canada

John D. Vienna
Pacific Northwest National Laboratory
Richland, WA 99352

ABSTRACT

A modified associate species thermochemical model has been developed for the liquid/glass in nuclear waste glass systems, and provides a simple means for relatively accurately representing the thermochemistry of the liquid/glass phase. A modification of the methodology is required when two immiscible liquids are present, such that a positive interaction energy is included in the representation. The approach has been extended to include spinel-forming constituents together with the base glass system as well as development of a models for spinel phases.

INTRODUCTION

The production of nuclear materials for defense applications at several sites in the United States over almost six decades has resulted in the accumulation of a substantial quantity of radioactive waste. These materials are currently stored in a variety of forms including liquids, sludges, and solids. In addition, there are similar wastes that have resulted from the reprocessing of commercial spent fuel, although this has occurred to a much smaller extent. While the composition and characteristics of the various high-level wastes (HLW) differ, their behavior is similar in many respects. The focus of current U. S. Department of Energy efforts with regard to permanent disposal of these materials is that they will be incorporated in a stable, insoluble host solid (a glass or specific crystalline phase).

Components such as Fe, Cr, Zr, and Al have limited solubility in HLW glasses (1-3). These components precipitate as oxide minerals such as spinel, zircon, and nepheline once their solubility in glass is exceeded. Precipitated minerals may cause melter failure (4) and can alter the physical properties such as the leach resistance of the glass (2). To avoid these problems, current HLW glasses are formulated to assure oxide minerals do not precipitate in the melter (2,5,6). The solubility of these components can dictate HLW glass volume produced at the Savannah River Site (7) and West Valley and to be produced at Hanford (5, 8).

Thermochemical assessment of the phase equilibria and modeling of the liquid/glass phase can support optimization of glass formulations with regard to stability and waste loading. In order to provide a sufficient thermochemical understanding of the liquid and glass system used for sequestering HLW, an approach using the associate species technique was chosen (9, 10). It is attractive because it (a) accurately represents the thermodynamic behavior of very complex chemical systems over wide temperature and composition ranges, (b) accurately predicts the activities of components in metastable equilibrium glass phases, (c) allows logical estimation of

unknown thermodynamic values with an accuracy much greater than that required for predicting useful engineering limits on thermodynamic activities in solutions, and (d) is relatively easy for non-specialists in thermochemistry to understand and use.

Ideal mixing of associate species accurately represent the solution energies in which end member components exhibit attractive forces. A modification to the associate species model, hence the term "modified" associate species model, is the incorporation of positive solution model constants to represent any positive interaction energies in a solution. With these it is possible to accurately represent reported immiscibility in solution phases (e.g., the liquid-liquid immiscibility common in many silica-containing systems). The results are simple, well-behaved equations for free energies that can be confidently extrapolated and interpolated into unstudied temperature and composition ranges. Thus, in support of the nuclear waste glass development effort, a model of the Na_2O-Al_2O_3-B_2O_3-SiO_2 was developed using the modified associate species approach and described elsewhere (9,10).

The work described here is focused on modeling spinel phases along with attendant liquid/glass and other crystalline phases in HLW systems. As noted above, previous efforts have successfully modeled the base glass system. Progress to date to include spinel-related constituents has resulted in modeling of the Fe-O, Mn-O, Al-Fe oxide, Cr-Fe oxide, and Al-Fe-Cr oxides. The basic data for the calculations are obtained from the 1996 version of the Scientific Group Thermodata Europe (SGTE) Pure Substance Database (12) and calculations are performed using the ChemSage (13) and FactSage (14) thermochemical software packages. Continuing efforts will seek to include other important elements in spinel phases, most notably Mn.

Fe-O SYSTEM

With the multivalent nature of iron and the importance of redox potential in many glass systems, the Fe-O system must be correctly modeled for its accurate inclusion in any liquid/glass system. This is less of an issue for HLW glass as efforts are made to fully oxidize species in the melter. Following the formalism described by Spear, et al. (9), liquid species' stoichiometry are chosen such that they contain 2 non-oxygen atoms per formula weight. The liquid/glass for Fe-O has been treated as a solution of Fe_2, Fe_2O_2, Fe_3O_4:2/3, and Fe_2O_3 species. The nomenclature for Fe_3O_4:2/3 indicates that the species has the Fe_3O_4 relative stoichiometry, although all values are multiplied by 2/3 in order to obtain 2 non-oxygen atoms per formula weight. The thermodynamic values for crystalline phases and liquid species were derived and are given in Tables I-IV. These were based on the SGTE database (12), the procedures described by Spear et al. (9), and from fitting published phase equilibria,. The liquid-liquid immiscibility of the Fe-O system, however, required that the solution be described using positive (repulsive) energetic terms. A simple Redlich-Kister (15) model, for which the values were manually fit to reproduce the phase equilibria, is adequate. It has the general formalism

$$G_{ex} = x_i x_j \Sigma (L_n (x_i - x_j)^{n-1} \quad \text{(J/mol)} \qquad (1)$$

where G_{ex} is the excess free energy of the solution, x_i and x_j are the mol fractions of species *i* and *j*, respectively. For the liquid phase the interacting species and interaction parameters are given in Table V.

Table I. Thermodynamic values for the crystalline phases based on the SGTE database and modified as necessary to develop associate species models. ($\Delta H_{f,298}$ is the 298K heat of formation, S_{298} is the 298K entropy, T is absolute temperature, T_{fus} is the melting temperature, and ΔH_{fus} is the heat of fusion.)

Crystalline Phase	$-\Delta H_{f,298}$(J/mol)	S_{298}(J/K-mol)	T_{fus}(K)	ΔH_{fus}(J/mol)
Mn	---	32.008	1517	12058.3
MnO	384928.	59.831	2058	54392.
Mn_3O_4	1386580.	153.971	1833	20920.
Mn_2O_3	956881.	110.458	---	decomposes
MnO_2	520071.	53.053	---	decomposes
Fe	---	27.280	1809	13807.2
FeO	279140.	43.2	1650	24058.
Fe_3O_4	1120000.	143.2	1870	138072.
Fe_2O_3	821500.	85.5	---	decomposes
Al_2O_3	1675692.	50.94	2327	111085.
Cr_2O_3	1150600.	81.1	2705	125000.
CrO_2	581576.	53.555	---	decomposes
Al_2FeO_4	1980870.	106.274	---	decomposes
$Al_2Fe_2O_6$	2405175.5	206.	---	decomposes
Cr_2FeO_4	1450760.	146.022	---	decomposes

Table II. Liquid species thermodynamic values based on the SGTE database and modified using the heat of fusion and fitting to the phase equilibria.

Liquid Species	$-\Delta H_{f,298}$(J/mol)	S_{298}(J/K-mol)
Mn_2	-20916.6	79.914
Mn_2O_2	658072.	172.517
Mn_3O_4:2/3	907440.	112.299
Mn_2O_3	955881.	110.458
Fe_2	-27614.	69.808
Fe_2O_2	475000.	134.5
Fe_3O_4:2/3	651000.	146.
Fe_2O_3	724000.	136.
Al_2O_3	581576.	53.555
Cr_2O_3	1015600.	127.3107
Al_2FeO_4:2/3	1309913.	70.84933
Cr_2FeO_4:2/3	955206.	97.348

Table III. Crystal phase SGTE-based heat capacity, transition temperature (T_{trans}), and heat of transition (ΔH^{o}_{trans}). Heat Capacity Coefficients: $C_p = a + b \bullet T + c \bullet T^2 + d/T^2$ (J/K-mol)

Phase	a	b	c	d	T_{trans}(K)	ΔH^{o}_{trans}(J/mol)
Mn	18.0891	0.0283786	-.928773E	-0548977.5	980	2225.9
	33.3004	0.435914E-02	0.0	0.0	1360	2121.3
	31.714701	0.8368E-02	0.0	0.0	1410	1878.6
	33.552799	0.82810E-02	0.0	0.0	1517	---
MnO.	46.484200	0.811696E-02	0.0	-368192.00	2115	---
Mn_3O_4	144.93401	0.04527090	0.0	-920480.	1445	---
Mn_2O_3	103.47000	0.0350619	0.0	-1351430.	1350	---
MnO_2	69.454399	0.010209	0.0	-1623390.	800	---
Fe	28.18	-7.32E-03	2.E-05	-290000.	1184	899.6
	28.	8.6E-03	0.0	0.0	1665	836.8
	24.64	9.9E-03	0.0	0.0	1809	---
FeO	48.	1.2E-02	-1.E-06	-200000.	1650	---
Fe_3O_4	153.55	5.E-02	0.0	0.0	700	0*
	175.	2.E-02	0.0	0.0	1184	0*
	165.	3.E-02	0.0	0.0	1870	---
Fe_2O_3	110.	5.E-02	0.0	-1700000.	700	0*
	138.	0.0	0.0	0.0	1050	0*
	130.	7.3E-03	-5.E-07	0.0	1980	---
Al_2O_3	117.49	1.038E-02	0.0	-3711000.	2327	---
Cr_2O_3	134.439	-.0126191	0.84377E-05	-2839800.	2705	---
CrO_2	48.534401	0.0118826	0.0	-1138050.	750	---
Al_2FeO_4	165.49	0.02238	-0.000001	-3911000.	1650	0*
	185.69	0.01038	0.0	-3711000.	2327	---
$Al_2Fe_2O_6$	227.49	0.06038	0.0	-5411000.	700	0*
	255.49	0.01038	0.0	-3711000.	1050	---
Cr_2FeO_4	182.439	-0.0006191	7.43775E-06	-3039800.	1650	0*
	202.639	-0.0126191	8.43775E-06	-2839800.	2705	---

*A value of zero for the enthalpy of transition indicates no transition occurs, but a new Cp equation is used for the next temperature range.

Table IV. Liquid species SGTE-based heat capacity, transition temperature (T_{trans}), and heat of transition (ΔH^{o}_{trans}). Heat Capacity Coefficients: $C_p = a + b \bullet T + c \bullet T^2 + d/T^2$ (J/K-mol)

Species	a	b	c	d	T_{trans}(K)	ΔH^{o}_{trans}(J/mol)
Mn_2	36.1782	0.0567572	-1.85755E-05	97955.	980	4451.8
	66.6008	0.00871828	0.0	0.0	1360	4242.6
	63.4294	0.016736	0.0	0.0	1410	3757.2
	67.1056	0.01656202	0.0	0.0	1517	fusion
	92.047996	0.0	0.0	0.0	2400	---
Mn_2O_2	92.9684	0.016233919	0.0	-736384.	2115	fusion
	121.335998	0.0	0.0	0.0	3000	---
Mn_3O_4:2/3	96.6227	0.0301806	0.0	-613653.3	1445	13947.
	140.0246667	0.0	0.0	0.0	1833	fusion
Mn_2O_3	103.47	0.0350619	0.0	-1351430.	1350	---
Fe_2	56.36	-1.464E-02	4.E-05	-580000.	1184	1799.2
	56.	1.72E-02	0.0	0.0	1665	1673.6
	49.28	1.98E-02	0.0	0.0	1811	fusion
	92.04	0.0	0.0	0.0	3000	---
Fe_2O_2	96.	2.4E-02	-2.E-06	-400000.	1650	fusion
	136.4	0.0	0.0	0.0	3000	---
Fe_3O_4:2/3	102.	3.33333E-02	0.0	0.0	700	0*
	116.667	1.33333E-02	0.0	0.0	1184	0*
	110.	2. E-02	0.0	0.0	1870	fusion
	133.888	0.0	0.0	0.0	3000	---
Fe_2O_3	110.	5. E-02	0.0	-1700000.	700	0*
	138.	0.0	0.0	0.0	1050	0*
	130.	7.3E-03	-5.E-07	0.0	1980	fusion
	148.	0.0	0.0	0.0	3000	---
Al_2O_3	117.49	1.038E-02	0.0	-3711000.	2327	0*
	192.464	0.0	0.0	0.0	3000	---
Cr_2O_3	134.439	-.0126191	0.84377E-05	-2839800.	2705	fusion
	170.	0.0	0.0	0.0	4500	---
Al_2FeO_4:2/3	110.3267	0.01492	-6.6667E-07	-2607333.	1650	0*
	123.7933	0.00692	0.0	-2474000.	2327	fusion
	173.776	0.0	0.0	0.0	3000	---
Cr_2FeO_4:2/3	121.626	-4.12733E-04	4.9585E-06	-2026533.	1650	0*
	135.0927	-0.008413	5.62517E-06	-1893200.	2705	fusion
	113.33333	0.0	0.0	0.0	4500	---

*A value of zero for the enthalpy of transition indicates no transition occurs, but a new Cp equation is used for the next temperature range.

Table V. G_{ex} coefficients (J/mol) (Eq. 1) for interacting species where T is absolute temperature.

Interacting Species	L_0	L_1	L_2
$Fe_2 – Fe_2O_2$	50,000	40,000	10,000
$Fe_2 – Fe_3O_4$	60,000	-	-
Fe_3O_4:2/3 – Fe_2O_3	25,000	-	-
$Mn_2 – Mn_2O_2$	100,000	50,000	-
Mn_3O_4:2/3 – Mn_2O_3	40,000	-	-
Al_2O_3 - Fe_2O_3	90,000 – 40T	-	-
Cr_2O_3 - Fe_2O_3	-80,000 + 10T	-30,000 + 10T	-

The published diagram of Fig. 1a compares well to the computed phase diagram seen in Fig. 1b. Unlike the simple, modified associate species model, the published diagram, which was also computed, utilized a compound energy model with ionic constituents for the crystalline phases and an ionic two-sublattice model (which required 8 polynomial expansions) for the liquid phases (16).

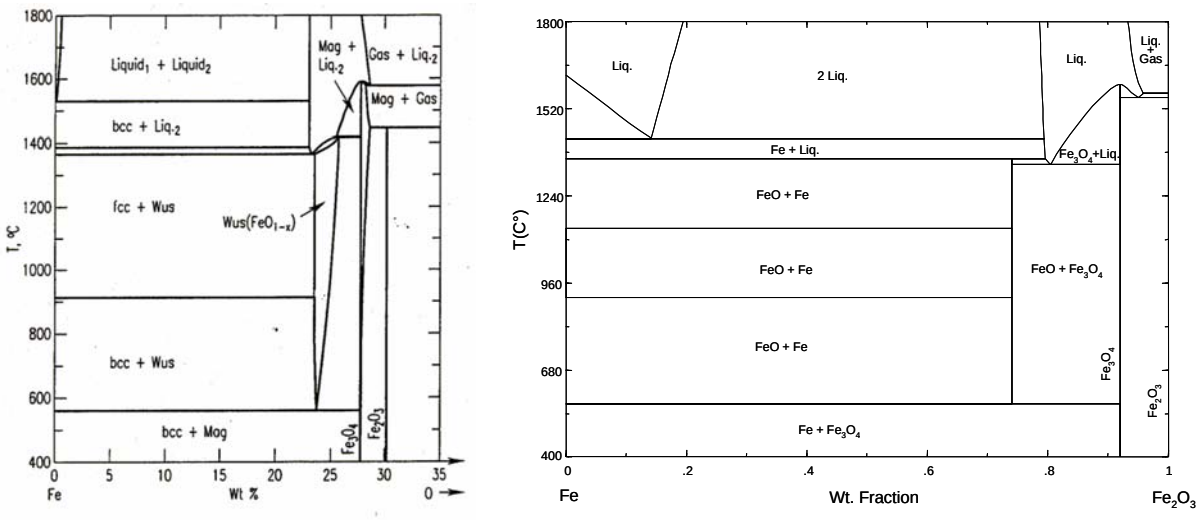

(a) (b)

Fig. 1. Fe-O phase diagram (a) computed by Sundman (16) and (b) computed in this work. (wus=wustite; mag=magnetite; bcc= body-centered cubic phase; fcc=face-centered cubic phase)

Mn-O SYSTEM

The Mn-O system, which is analogous to the Fe-O system, was approached in a similar manner. The liquid/glass phase was treated as a solution of Mn_2, Mn_2O_2, Mn_3O_4:2/3, and Mn_2O_3 species having the thermodynamic values listed in Table I-IV. The system also exhibits liquid-liquid immiscibility. The necessary interaction energy terms for the Redlich-Kister (15) excess free energy that were derived are listed in Table V. The published phase diagram, which was

determined in the same manner as the published Fe-O diagram (18), is seen in Fig. 2a and reasonably reproduces the computed diagram of this work seen in Fig. 2b.

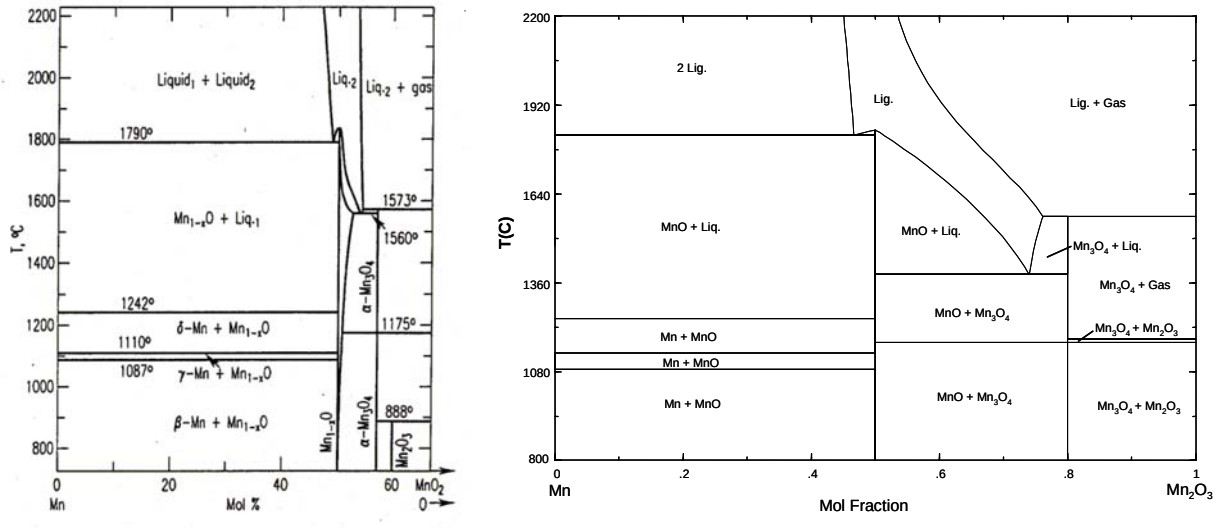

(a) (b)

Fig. 2. Mn-O phase diagram (a) computed by Wang and Sundman (18) and (b) computed in this work.

Al-Fe OXIDE LIQUID/GLASS, SESQUIOXIDE, AND SPINEL

The alumina-iron oxide solution that represents the liquid/glass is made up of the species: Al_2O_3, Fe_2, Fe_2O_2, Fe_3O_4:2/3, Fe_2O_3, $FeAl_2O_4$:2/3. No additional interaction parameters were used beyond those for the unary systems and only one binary oxide associate was included.

The two-sublattice model (19) was used for the spinel phase, with an excess energy for the interactions between Fe^{3+} and Al^{3+} on the sublattice of

$$G_{xs} = x_{Fe3+} \cdot x_{Al3+} \cdot A \qquad \text{(j/mol)} \qquad (2)$$

where x is the concentration of the subscripted atom on the sublattice and A=20 kj/mol. In addition, adjustments were necessary to the 298 K heat of formation and entropy of the $AlFeO_3$ phase.

The sesquioxide phases, hematite and corundum, required the zeroth-order Redlich-Kister (15) interaction parameters (Eq. 1) shown in Table V to adequately represent the end-member solution phases.

The experimental diagram is seen in Figure 3a (20) and can be compared with the computed phase diagram of Figure 3b. The model does not reproduce all the details accurately, but given the sparsity of data and the reasonable agreement in temperature, it is a good fit.

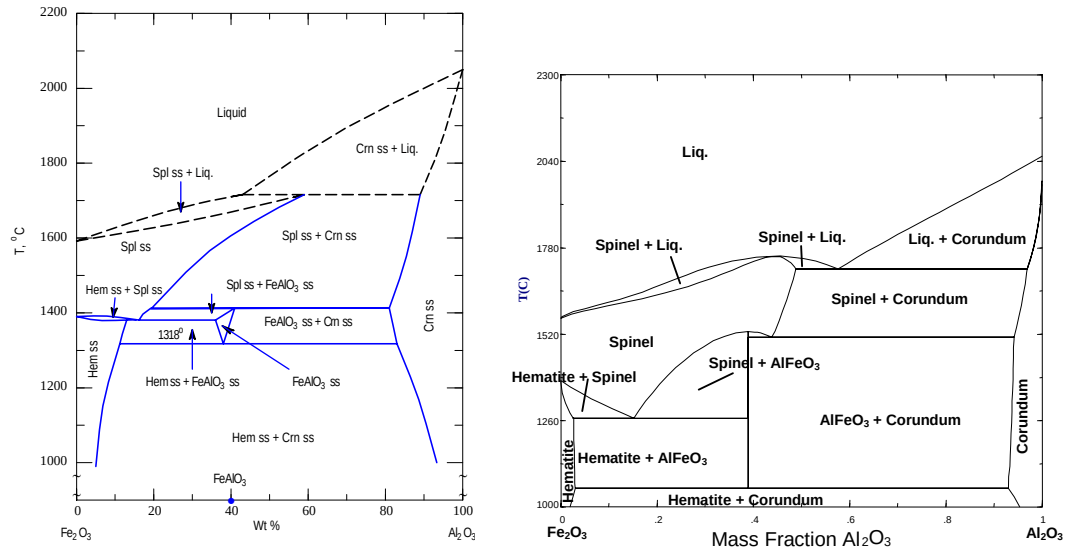

(a) (b)

Fig. 3. Al_2O_3-Fe_2O_3 phase diagram (a) of Muan and Gee (20) and (b) computed in this work.

Cr-Fe OXIDE LIQUID/GLASS, SESQUIOXIDE, AND SPINEL

The chromia-iron oxide solution that represents the liquid/glass is treated very similarly to that of the alumina-iron oxide solution, made up of the species: Cr_2O_3, Fe_2, Fe_2O_2, Fe_3O_4:2/3, Fe_2O_3, $FeCr_2O_4$:2/3. Again, no additional interaction parameters were used beyond those for the unary systems and only one binary oxide associate was included.

The two-sublattice model (19) was used for the spinel phase, with an excess energy for the interactions between Fe^{3+} and Cr^{3+} on the sublattice of A=8 kj/mol (Eq. 2). The sesquioxide solution phase required zeroth- and first-order Redlich-Kister (15) (Eq. 1) interaction parameters (Table V) to adequately represent the end-member solution phases. The experimental diagram is seen in Fig. 4a (21) and can be compared with the computed phase diagram of Figure 4b. The model reproduces the essential phase equilibria, but disagrees significantly in the uncertain area of the liquidus.

Al_2O_3-Cr_2O_3-Fe_2O_3 PHASE EQUILIBRIA

The systems described above were combined to obtain a model for the alumina-chromia-iron oxide system and it includes all the liquid/glass species and interaction parameters, as well as all crystalline phases. No ternary associates were used in the model as well as no additional interaction parameters. An example phase diagram at 1500°C was computed and can be seen in Fig. 5 compared to an experimentally determined diagram (22). While the phase regions do not completely match, again the major features are correct and the results can be considered good for so simple an approach.

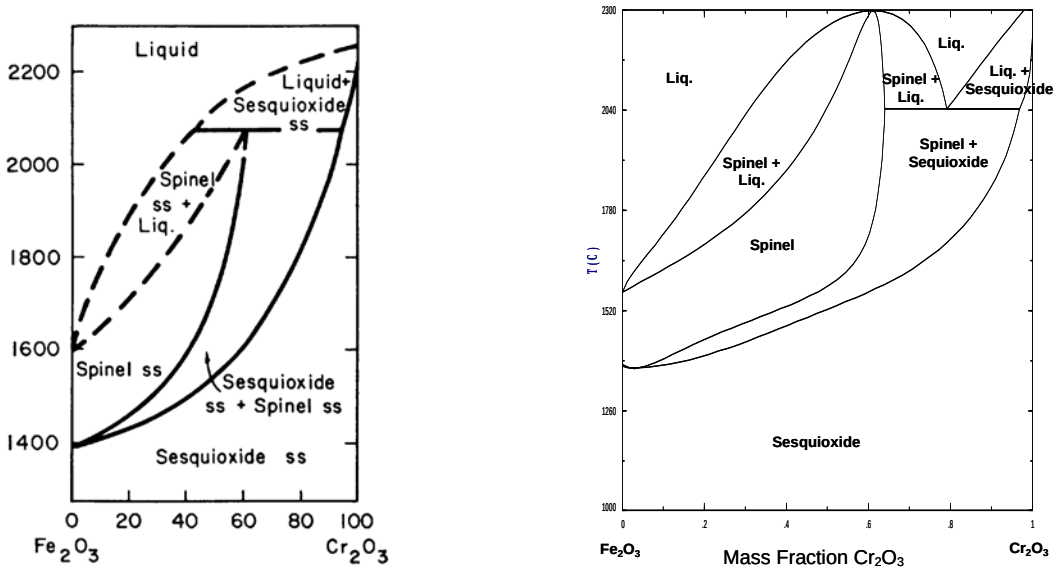

(a) (b)

Fig. 4. Cr_2O_3-Fe_2O_3 phase diagram (a) of Muan and Somiya (21) (b) computed in this work.

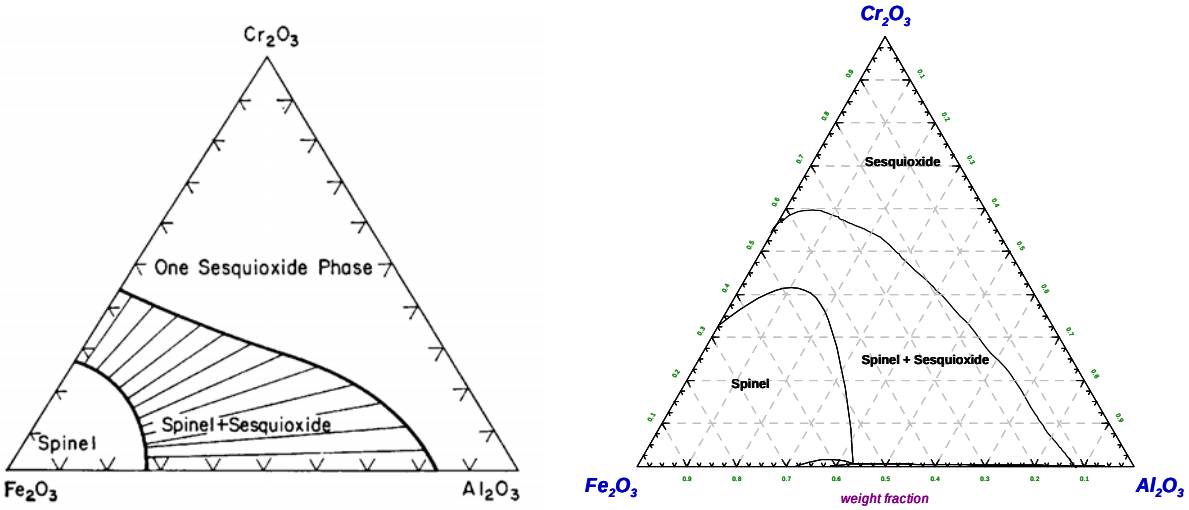

(a) (b)

Fig. 5. Al_2O_3-Cr_2O_3-Fe_2O_3 phase diagram (a) of Muan and Somiya (22) (b) computed in this work.

CONCLUSIONS

The modified associate species approach for complex systems is simple, relatively accurate, and highly usable for describing liquidus surfaces, conditions for crystalline phase formation, and chemical activities of glass constituents. A base model for HLW glass systems that agrees reasonably with published phase diagrams has been developed. The very simple and usable modeling approach has successfully described important features of the Fe-O and Mn-O systems.

Efforts to similarly model the Cr_2O_3-Fe_2O_3 and Al_2O_3-Fe_2O_3 systems have been reasonably successful. The results have been combined to provide a comprehensive model of the alumina-chromia-iron oxide system.

ACKNOWLEDGMENTS

The authors thank T.R. Watkins and M.J. Lance for their useful comments. Research supported by the DOE Office of Biological and Environmental Research, U.S. Department of Energy, under Contract DE-AC05-00OR22725 with Oak Ridge National Laboratory, managed and operated by UT-Battelle, LLC.

REFERENCES

1. P. Hrma, G.F. Piepel, M.J. Schweiger, D.E. Smith, D.S. Kim, P.E. Redgate, J.D. Vienna, C.A. LoPresti, D.B. Simpson, D.K. Peeler, M.H. Langowski, "Property / Composition Relationships for Hanford High-Level Waste Glasses Melting at 1150°C"; PNL-10359, , Pacific Northwest Laboratory, Richland, WA, Vol. 1 and 2, 1994.

2. K.S. Kim, D.K. Peeler, and P. Hrma, "Effects of Crystallization on the Chemical Durability of Nuclear Waste Glasses," *Ceramic Transactions* **61** 177-85 (1995).

3. M. Mika, M.J. Schweiger, J.D. Vienna, P. Hrma, "Liquidus Temperature of Spinel Precipitating High-Level Waste Glasses," pp. 71-78 in *Scientific Basis for Nuclear Waste Management XX*, Edited by W.J. Gray, I.R. Triay, MRS Processing Vol. 465; Materials Research Society: Warrendale, PA, 1990;.

4. D.F. Bickford, A. Applewhite-Ramsey, C.M. Jantzen, K.G. Brown, "Control of Radioactive-Waste Glass Melters. 1. Preliminary General Limits At Savannah River," *Journal of the American Ceramic Society* **73**, 2896-2902 (1990).

5. P. Hrma, J. D. Vienna, and M. J. Schweiger, "Liquidus Temperature Limited Waste Loading Maximization for Vitrified HLW," *Ceramic Transactions*,**72** 449-56 (1996).

6. J.D. Vienna, P. Hrma, M.J. Schweiger, D.E. Smith, D.S. Kim, "Low-Temperature High-Waste Loading Glass for Hanford DST/SST High-Level Waste Blend - Technical Note," PNNL-11126, Pacific Northwest Laboratory, Richland, WA, 1995.

7. P. Hrma, J.D. Vienna, M. Mika, J.V. Crum, T.B. Edwards, "Liquidus Temperature Data for DWPF Glass," PNNL-11790, Pacific Northwest National Laboratory, Richland, WA, 1998.

8. S.L. Lambert, G.E. Stegen, J.D. Vienna, "Tank Waste Remediation System Phase I High-Level Waste Feed Processability Assessment Report," WHC-SD-WM-TI-768, Westinghouse Hanford Company, Richland, WA, 1996.

9. K.E. Spear, T.M. Besmann, and E.C. Beahm, "Thermochemical Modeling of Glass: Application to High-Level Nuclear Waste Glass," *MRS Bulletin*, **24** [4] 37-44 (1999).

10. T.M. Besmann and K.E. Spear, "Thermochemical Modeling of Oxide Glasses," J*ournal of the American Ceramic Society*, **85** 2887-94 (2002).

12. A.T. Dinsdale, "SGTE Data for Pure Elements," *Calphad* **15** 317-425 (1991).

13. G. Eriksson, and K. Hack, "ChemSage - A Computer Program for the Calculation of Complex Chemical Equilibria," *Metallurgical Transactions B*, **21B** 1013-23 (1990).

14. C.W. Bale, P. Chartrand, S.A. Degterov, G. Eriksson, K. Hack, R. Ben Mahfoud, J. Melançon, A.D. Pelton, S. Petersen, "FactSage thermochemical software and databases" *CALPHAD*, **26** 189-228 (2002).

15. M. Hillert, *Phase Equilibria, Phase Diagrams, and Phase Transformations*, Cambridge University Press, NY, p. 462 (1998).

16. B. Sundman, “An Assessment of the Iron-Oxygen System,” *Journal of Phase Equilibria*, **12** 127-40 (1991).

18. M.S. Wang, B. Sundman, “Thermodynamic Assessment of the Mn-O System,” *Metallurgical Transactions B*, **23B** 821-31 (1992).

19. A. D. Pelton, H. Schmalzried, and J. Sticher, “Thermodynamics of Mn_3O_4-Co_3O_4, Fe_3O_4-Mn_3O_4, and Fe_3O_4-Co_3O_4 Spinels by Phase Diagram Analysis,” *Ber. Nunsenges. Phys. Chem.*, **83** 241-52 (1979).

20. A. Muan and C.L. Gee, “Phase Equilibrium Studies in the System Iron Oxide-Alumina in Air and at One Atmosphere Oxygen Pressure,” *Journal of the American Ceramic Society*, **39** 207-14 (1956).

21. A. Muan and S. Somiya, “Phase Relations in the System Iron Oxide-Cr_2O_3 in Air,” *Journal of the American Ceramic Society*, **43** 204-9 (1960).

22. A. Muan and S. Somiya, “Phase Equilibrium Studies in the System Iron Oxide-Al_2O_3-Cr_2O_3,” *Journal of the American Ceramic Society*, **42** 603-13 (1959).